Supporting Information

Maglia *et al.* 10.1073/pnas.0808296105

SI Text

SI Methods

Protein Preparation. αHL was produced as described elsewhere (1). In short, the protein was expressed in the presence of [^{35}S]methionine in an *E. coli in vitro* transcription and translation (IVTT) system (*E. coli* T7 S30 Extract System for Circular DNA, catalog no. L1130, Promega). IVTT reactions (100 μl) containing αHL monomers were incubated with rabbit red blood cell membranes for 1 h at 37 °C. The solution was spun at 25,000 × *g* and the pellet containing αHL heptamers was loaded onto a 5% SDS-polyacrylamide gel. The gel was run for 4 h at 100 V and vacuum dried for 3 to 4 h without heating onto Whatman 3M filter paper. The dried gel was exposed to photographic film for 2 h and the developed film was used to locate the position of the heptameric protein in the gel. This region of the gel was cut out, rehydrated and crushed in 400 μl of 10 mM Tris.HCl, pH 8.0, containing 100 μM EDTA. After 20 min at room temperature, the polyacrylamide was removed by centrifuging the suspension at 25,000 × *g* for 7 min at room temperature through a cellulose micro spin column (Microfilterfuge tubes, catalog no. 7016-024, Rainin). Aliquots of the purified protein were stored at −80 °C.

Mutant αHL genes were prepared either by using a site-directed mutagenesis kit (QuikChange II XL, catalog no. 200522–5, Stratagene) or by cassette mutagenesis (2). The RL2 gene encodes four amino acid replacements in the barrel domain (Val-124 → Leu, Gly-130 → Ser, Asn-139 → Gln, Ile-142 → Leu) and one in the amino latch region of the pore (Lys-8 → Ala) (2). The DNA sequence of each new gene was verified.

Planar Bilayer Recordings. A bilayer of 1,2-diphytanoyl-*sn*-glycero-3-phosphocholine (Avanti Polar Lipids) was formed on an aperture (≈100 μm in diameter) in a 25-μm thick polytetrafluoroethylene film (Goodfellow Cambridge Limited, catalog no. FP301200/10) that divided a chamber into *cis* and *trans* compartments. Both compartments contained 0.4 ml of 1 M KCl, 25 mM Tris.HCl, pH 8, containing 100 μM EDTA. Planar bilayer current recordings were performed with a patch clamp amplifier (Axopatch 200B, Axon Instruments). The protein and subsequently the DNA were added to the *cis* compartment, which was connected to ground. The DNA was prepared and PAGE-purified by Sigma–Genosys. The concentration of the DNA was determined by measuring the absorbance at 260 nm of the solution in the *cis* chamber at the end of each experiment. The DNA sequence was: 5′-AAAAAAAAAAAAAAAAAAAATTCCCCCCCCCC-CCCCCCCCCCCCTTAAAAAAAAAATTCCCCCCCCCC-TTAAAAAAAAAATTCCCCCCCCCC-3′. At applied potentials above +120 mV, the amplified signal arising from the ionic current passing through the αHL pore was low-pass filtered at 50 kHz and sampled at 250 kHz with a computer equipped with a Digidata 1440A digitizer (Molecular Devices). At applied potentials of +100 mV and +80 mV the signal was filtered at 40 kHz, whereas at +60 mV and +40 mV the signal was filtered at 30 kHz and 20 kHz, respectively. The sampling rate was at least five times the filtering rate.

Under the conditions of the experiments, all of the mutant pores exhibited a stable open-pore current with only occasional current spikes due to transient gating. For example, the mutant that had the highest level of gating, E111N-WT, showed short and long endogenous current blockades. The short spikes, defined by no more than a couple of data points, occurred at ≈0.1 s^{-1}. The long blockades were rarer (≈0.01 s^{-1}) and often resulted in a full block of the pore, which was relieved by stepping the applied potential between high positive and negative values.

The data used in Table 2 were analyzed with pClamp 10.1 software (Axon Instruments), by using three different current levels. Level 0 corresponded to the open channel current, level 1 to the mid-amplitude event current and level 2 to the low-amplitude event current. The assignment to each level was checked manually. The data used in Fig. 2*B* were analyzed and prepared for presentation by using only two levels: level 0 was set to the open channel current, and level 1 was placed between the mid-amplitude and low-amplitude event currents. The frequency of DNA translocations was calculated by fitting the interevent intervals to a single exponential (logarithmic binning, 10 bin/decade) and normalizing the mean value of the duration to a DNA concentration of 1 μM. The DNA translocation time was calculated from the peak of a histogram of the distribution of the translocation times (3).

Curve Fitting. The values of f_{max}, b, and V_0 (Table S1) were determined by fitting the voltage dependence of the frequency of DNA translocation for the WT and mutated αHL nanopores to Eq. **1** (Fig. 5) by using Origin data analysis software (OriginLab). The errors in these values are expressed as standard errors. The curve fittings were adjusted for the experimental error of each point by using the instrumental weight.

SI Results and Discussion

Dwell-Time/Amplitude Distributions of the Events for M113R-WT and E111N-WT. Dwell-time/amplitude distributions of the events for the M113R-WT and E111N-WT homoheptamers (but not the other mutants) yielded two distinct clusters of current blockades at +100 to +200 mV (Fig. S4). The relative intensities of the two peaks in the distributions were voltage dependent, with the proportion of longer events increasing with the applied potential (Fig. S4*c*). The first peak comprised blockades with a short dwell time and a fractional residual current at +120 mV of 0.04 for M113R-WT and 0.11 for E111N-WT. The second cluster of current blockades included events with a longer dwell time and almost full current block. It is unlikely that the two clusters can be accounted for by 5′ versus 3′ threading (4), because the differences in dwell times are too great (≈100-fold).

In this study, the blockades at +120 mV are considered. At this potential, the short-lived events dominate in the dwell-time/amplitude distributions for M113R-WT and E111N-WT and it is these events, which are predominantly type A (Table 2), that are considered. To determine the frequency of DNA translocation both short and long events were included, but the contribution of the latter is minor.

Assignment of Intermediate *V*. The assignment of intermediate *V* is supported by the findings of Kasianowicz and coworkers, who showed that, under a positive applied potential, the *cis* addition of ssDNA produces short lived current blockades of 85–100% of the open pore current. PCR analysis of the *trans* chamber revealed that DNA had passed through the αHL nanopore (5). Further, Movileanu and colleagues observed that individual PEG molecules covalently attached inside the β barrel produce a much higher reduction of the open pore current (70%) than when they are attached within the vestibule (20%) (6). Howorka and Bayley found that DNA duplexes covalently attached near the *cis* entrance with overhangs that protrude into the β barrel produce a current

reduction of ≈90% of the open pore current (7). Finally, DNA immobilized inside the β barrel as part of a DNA-αHL rotaxane structure causes a 85% block of the pore current (8).

Assignment of the Mid-Level Events. Occupancy of the vestibule is associated with a reduced conductance (but not to the extent caused by occupancy of the barrel). For example, when high molecular weight PEG molecules (6) or PAMAM dendrimers with a hydrodynamic diameter of 4.1 nm (9) are tethered within the vestibule, the current is reduced by 20% and 45%, respectively. Second, when DNA duplexes are tethered within the vestibule, a 38% reduction of the pore current is observed (7). Finally, when the αHL pore was genetically engineered so that the vestibule was filled with flexible polypeptides chains, the current was reduced by up to 70%, the reduction depending on the number of amino acids inserted (10).

1. Cheley S, Braha O, Lu X, Conlan S, Bayley H (1999) A functional protein pore with a ''retro'' transmembrane domain. *Protein Sci* 8:1257–1267.
2. Cheley S, Gu L-Q, Bayley H (2002) Stochastic sensing of nanomolar inositol 1,4,5-trisphosphate with an engineered pore. *Chem Biol* 9:829–838.
3. Meller A, Nivon L, Brandin E, Golovchenko J, Branton D (2000) Rapid nanopore discrimination between single polynucleotide molecules. *Proc Natl Acad Sci USA* 97:1079–1084.
4. Mathé J, Aksimentiev A, Nelson DR, Schulten K, Meller A (2005) Orientation discrimination of single-stranded DNA inside the alpha-hemolysin membrane channel. *Proc Natl Acad Sci USA* 102:12377–12382.
5. Kasianowicz JJ, Brandin E, Branton D, Deamer DW (1996) Characterization of individual polynucleotide molecules using a membrane channel. *Proc Natl Acad Sci USA* 93:13770–13773.
6. Movileanu L, Cheley S, Howorka S, Braha O, Bayley H (2001) Location of a constriction in the lumen of a transmembrane pore by targeted covalent attachment of polymer molecules. *J Gen Physiol* 117:239–251.
7. Howorka S, Bayley H (2002) Probing distance and electrical potential within a protein pore with tethered DNA. *Biophys J* 83:3202–3210.
8. Sánchez-Quesada J, Saghatelian A, Cheley S, Bayley H, Ghadiri MR (2004) Single molecule DNA rotaxanes of a transmembrane pore protein. *Angew Chem Int Ed* 43:3063–3067.
9. Martin H, *et al.* (2007) Nanoscale protein pores modified with PAMAM dendrimers. *J Am Chem Soc* 129:9640–9649.
10. Jung Y, Cheley S, Braha O, Bayley H (2005) The internal cavity of the staphylococcal α-hemolysin pore accommodates ≈175 exogenous amino acid residues. *Biochemistry* 44:8919–8929.

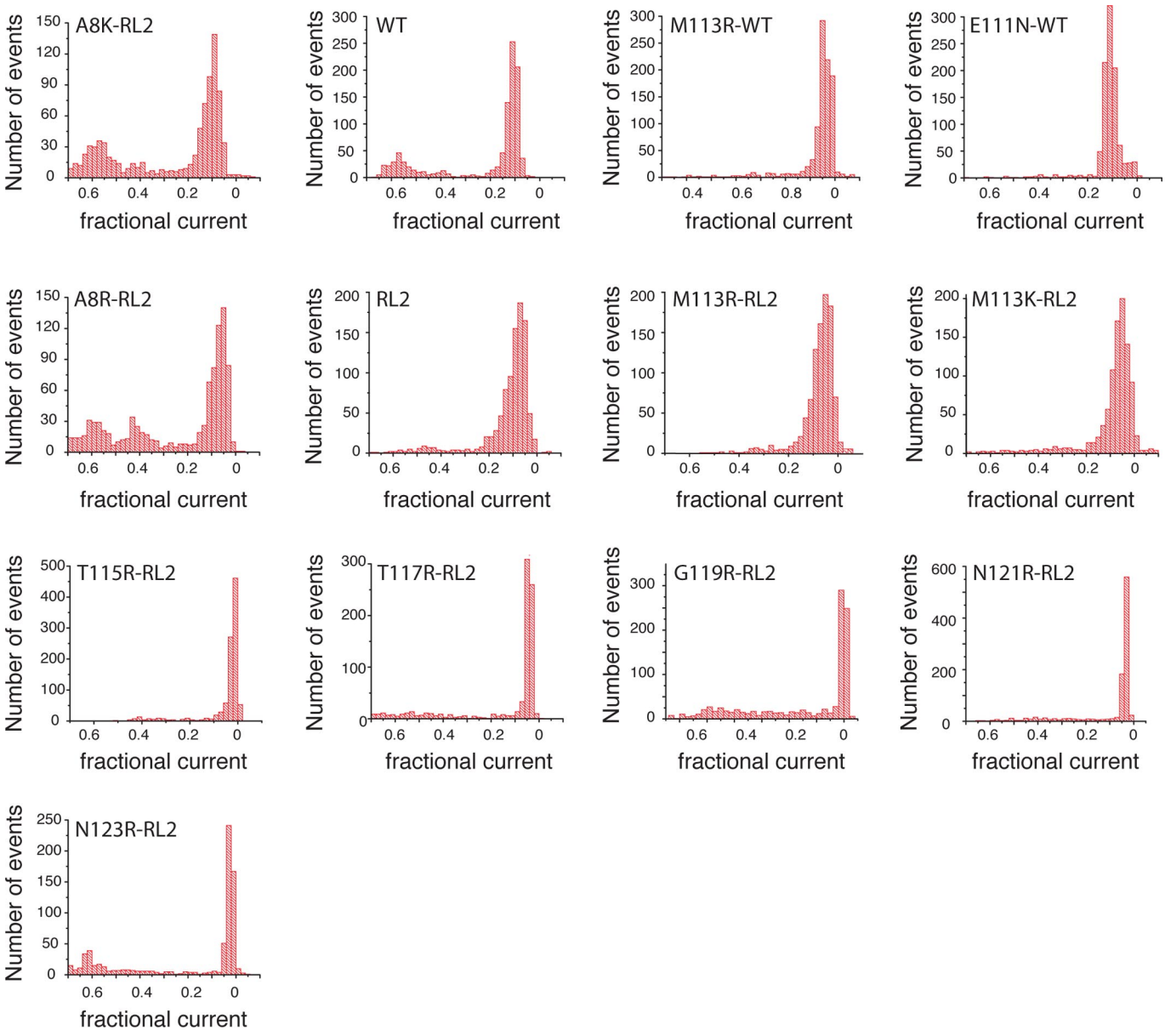

Fig. S1. Amplitude histograms of mean event currents for DNA blockades of various αHL pores. The main peak represents the type A events (DNA translocation). Each plot comprises 1000 events. The conditions are described in the legend to Fig. 2.

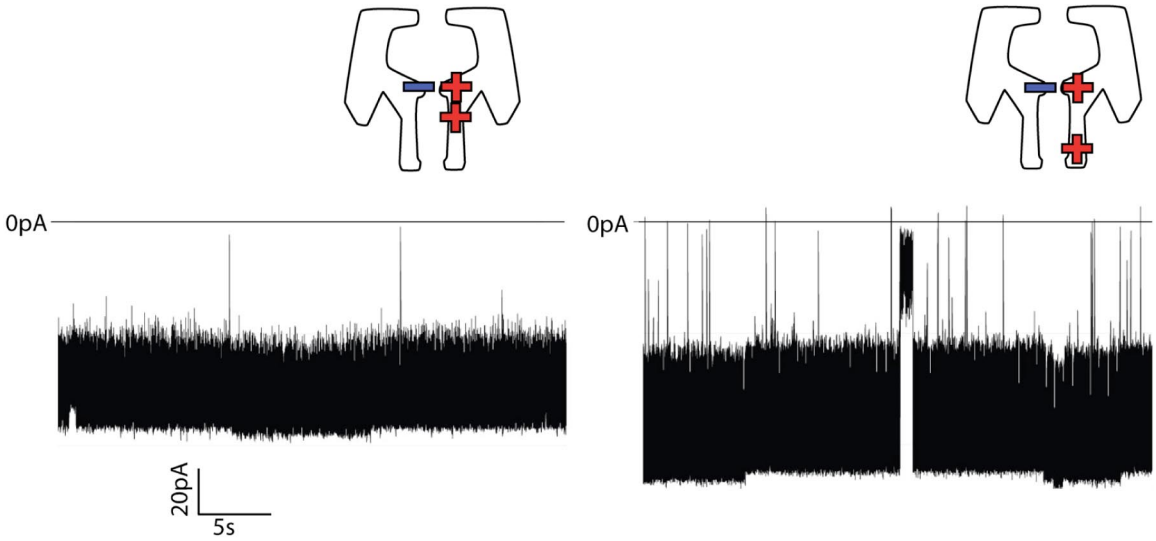

Fig. S2. Current blockades after DNA addition (1.0 μM) to the *trans* chamber for: (*a*) M113R-RL2 and (*b*) N121R-RL2. The applied potential was −120 mV. For these mutants the currents through the open pores are much noisier at negative potentials than at positive potentials. Further conditions are described in the legend to Fig. 2.

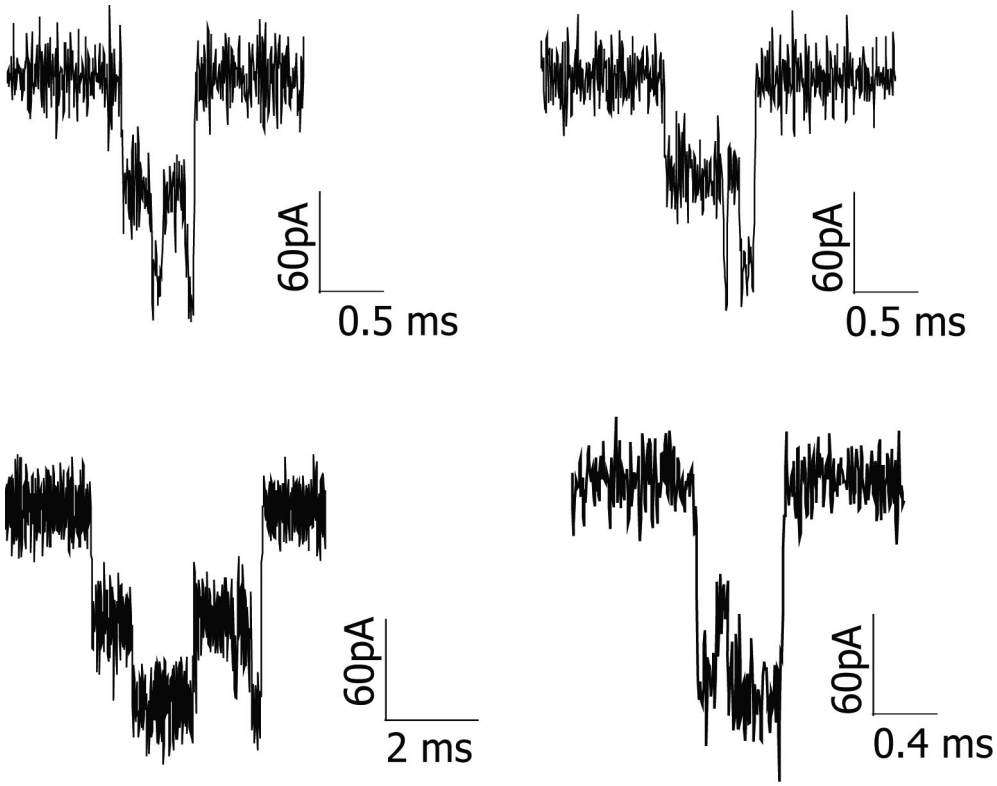

Fig. S3. Rare (<1%) current blockade events for DNA translocation through WT-αHL nanopores at +120 mV showing multiple transitions between the mid-amplitude and low-amplitude states. The conditions are described in the legend to Fig. 2.

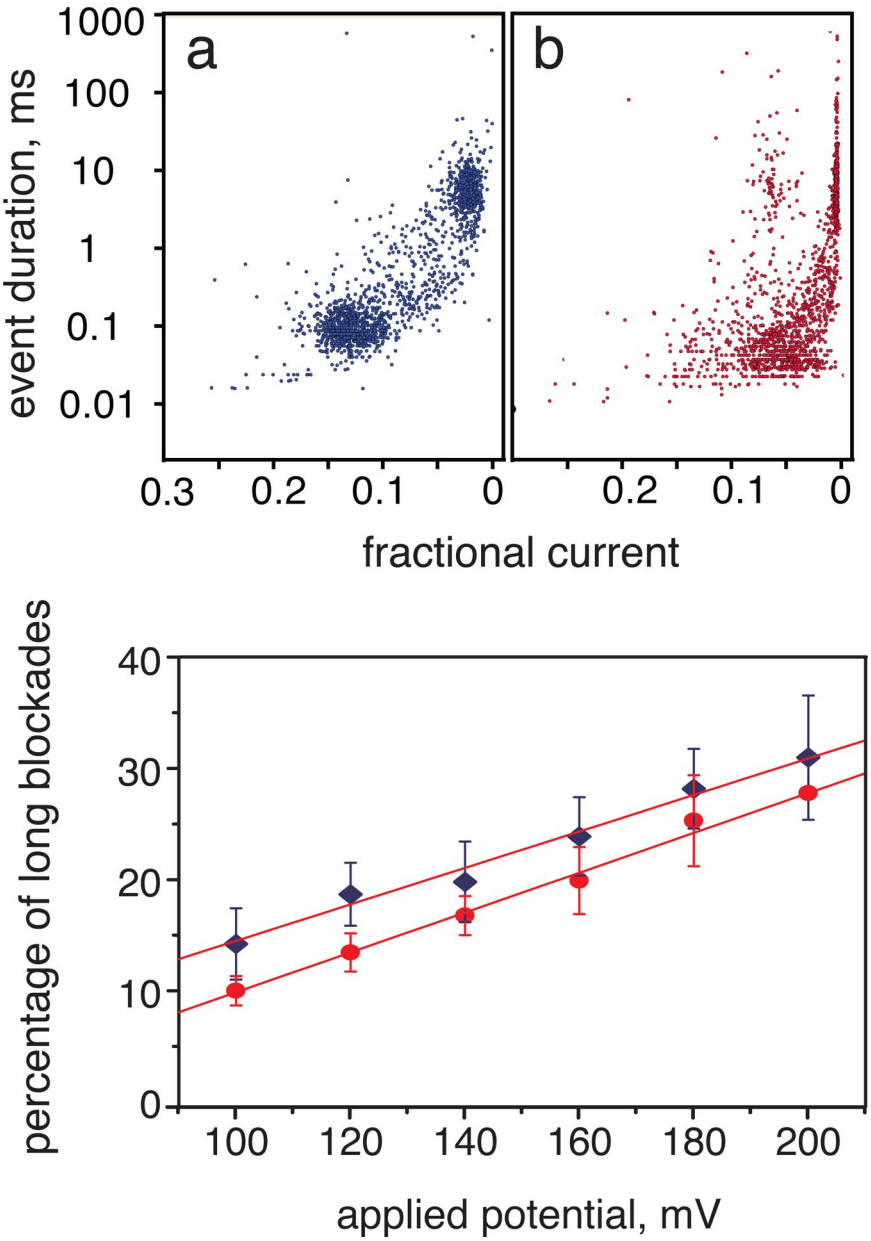

Fig. S4. DNA blockades for the homoheptameric mutant αHL pores E111N-WT and M113R-WT. (*a*) Currents through E111N-WT during DNA-induced blockades at +200 mV, expressed as a fraction of the open-pore current, versus the event duration displayed on a semilogarithmic scale. (*b*) Corresponding plot for M113R-WT. (*c*) Long blockades for E111N-WT (blue diamonds) and M113R-WT (red circles) as a percentage of the total for applied potentials from +100 to +200 mV. The DNA was added to the *cis* chamber at $\approx$0.5 μM; the exact concentration was determined after each experiment. For further conditions, see Fig. 2.

Table S1. Values of f_{max}, b, and V_0 for various αHL pores

αHL pore	f_{max}	b	V_0	V_1
M113R-WT	7,300 ± 2,200	1200 ± 100	−90 ± 7	45
E111N-WT	1,600 ± 200	780 ± 40	−56 ± 3	50
M113R-RL2	990 ± 300	990 ± 90	−67 ± 7	77
WT	300 ± 60	420 ± 40	25 ± 6	100
RL2	300 ± 150	980 ± 130	20 ± 17	151

The values were derived by fitting the data to equation 1 (see Methods). Additional conditions are described in the legend to Fig. 2. V_1 is the potential at which the normalized frequency of translocation is 1 $s^{-1}\cdot\mu M^{-1}$.